Serb. Astron. J. № 204 (2022), 29 - 38
DOI: https://doi.org/10.2298/SAJ2204029F

UDC 524.7–823 + 524.8
Original scientific paper

LARGE-SCALE HOMOGENEITY IN THE DISTRIBUTION OF QUASARS IN THE HERCULES-CORONA BOREALIS GREAT WALL REGION

Hirokazu Fujii

Independent Researcher, Minato-ku, Tokyo, Japan
E–mail: *hirokazufujii@gmail.com*

(Received: September 27, 2021; Accepted: February 23, 2022)

SUMMARY: In light of recent debates on the existence of a gigaparsec-scale structure traced by gamma-ray bursts, namely the Hercules-Corona Borealis Great Wall (HCBGW), we revisit large-scale homogeneity in the spatial distribution of quasars. Our volume-limited sample of quasars in the redshift range $1.6 < z \leq 2.1$, which is constructed from the data release 7 of the Sloan Digital Sky Survey quasar catalogue, covers about half of the suspected HCBGW region. We analyze the sample in two complementary ways: fractal analysis of determining the average scale of homogeneity and friends-of-friends analysis of identifying specific large-scale structures. The quasar distribution on average reaches homogeneity at $r_{\rm h} = 136 \pm 38h^{-1}$ Mpc and the richness and comoving size frequencies of large ($\gtrsim 150h^{-1}$ Mpc) quasar groups are consistent with the prediction of homogeneous distribution. These results put constraints on the spatial extent of the HCBGW but do not contradict its existence since our quasar sample does not cover the entire HCBGW region.

Key words. Quasars: general – Cosmology: large-scale structure of Universe

1. INTRODUCTION

The cosmological principle is the hypothesis that the universe is homogeneous and isotropic if averaged over a sufficiently large scale, which allows us to describe the background geometry of spacetime by the Friedmann-Lemaître-Robertson-Walker (FLRW) metric. It is a crucial assumption in the concordance Lambda Cold Dark Matter (ΛCDM) model, a variety of spatially flat FLRW general relativistic cosmologies (e.g. Ellis et al. 2012).

The homogeneity scale is a comoving length scale above which the distribution of cosmic matter looks uniform within a certain precision. Statistical studies of the spatial distribution of galaxies and quasars have shown that the homogeneity scale should lie within $70h^{-1}$ Mpc and $200h^{-1}$ Mpc (e.g. Pan and Coles 2000, Hogg et al. 2005, Sarkar et al. 2009, Scrimgeour et al. 2012, Laurent et al. 2016, Ntelis et al. 2017, Gonçalves et al. 2018a,b, Gonçalves et al. 2021), which is consistent with the theoretical upper limit $\approx 260h^{-1}$ Mpc for the ΛCDM model (Yadav et al. 2010). However, some authors argue that the current observational data do not show homogeneity even on the largest scales explored thus far (e.g. Joyce et al. 1999, Sylos Labini et al. 2009, Sylos Labini 2011, Sylos Labini et al. 2014, Park et al. 2017).

The existence of cosmic structures (i.e. filaments and walls traced by galaxies and quasars) larger than the homogeneity scale has often been claimed to be evidence against the cosmological principle (Sheth and Diaferio 2011, Clowes et al. 2012, 2013). However, subsequent studies have shown that such structures can be formed in a ΛCDM universe (Park et al. 2012, Marinello et al. 2016), or that they are not even physical structures but merely patterns created by chance (Nadathur 2013, Pilipenko and Malinovsky 2013, Einasto et al. 2014, Park et al. 2015). The lat-

est report by Lopez et al. (2022) on the discovery of a gigaparsec-scale arc-like structure would also need to be examined in more detail.

In recent years, the accumulating redshift data of distant gamma-ray bursts (GRBs) have revealed the possible existence of other gigantic structures. The so-called Hercules-Corona Borealis Great Wall (HCBGW) spanning about 3 Gpc in the redshift range $1.6 < z \leq 2.1$ is one example (Horváth et al. 2014, 2015, 2020), the Giant GRB Ring of diameter 1.7 Gpc at $0.78 < z < 0.86$ is another (Balázs et al. 2015, 2018). These associations of GRBs greatly exceed in size the predicted upper limit of the homogeneity scale $260h^{-1}$ Mpc (Yadav et al. 2010), and their existence may not reconcile with the cosmological principle (Mészáros 2019). The HCBGW has also attracted attention as a candidate for the largest structure possible in the screening of gravity (Eingorn 2016, Canay and Eingorn 2020).

However, there is debate about the statistical significance of the HCBGW. Ukwatta and Woźniak (2016) argued that the anisotropic distribution of GRBs at the location of the HCBGW can be accounted for by nonuniform exposure times over the sky of the Neil Gehrels Swift Observatory. Christian (2020) investigated in detail the validity of the statistical methods employed by Horváth et al. (2014, 2015) and concluded negatively. Although Horváth et al. (2020) countered these papers, they also admit that the currently available GRB data are not sufficient to confirm the existence of the HCBGW.

If the HCBGW is a physical structure, it should also affect the distribution of cosmic objects other than GRBs. In this context, we explore large-scale homogeneity in the spatial distribution of quasars at redshifts $1.6 < z \leq 2.1$, which are taken from the data release 7 (DR7) of the Sloan Digital Sky Survey (SDSS) quasar catalogue (Schneider et al. 2010). Nadathur (2013), Pilipenko and Malinovsky (2013), Einasto et al. (2014) and Park et al. (2015) performed similar tests using the same catalogue, but they used quasars at redshifts $z \leq 1.8$. Our quasar sample covers about half of the area where the HCBGW is supposed to lie.

The paper is organized as follows. In Section 2, we define the term "HCBGW region", i.e. the location and extent of the HCBGW, following the method of Horváth et al. (2014, 2015, 2020). In Section 3, we construct a volume-limited uniform sample of quasars that covers about half of the identified HCBGW region. Using this sample, we perform a fractal analysis to measure the homogeneity scale (Section 4) and a friends-of-friends analysis to study specific large-scale structures (Section 5). Discussion and conclusion are given in Section 6.

Throughout the paper, we assume the concordance ΛCDM cosmology with density parameters $\Omega_{\rm m} = 0.3$, $\Omega_\Lambda = 0.7$ and the Hubble-Lemaître constant $H_0 = 100h$ km s^{-1} Mpc^{-1} with $h = 0.7$.

2. THE SUSPECTED HCBGW REGION

The possible existence of the HCBGW has been claimed by Horváth et al. (2014, 2015, 2020) on the basis of an unusually large (on a scale of $\sim 50°$) clustering of GRBs at redshifts $1.6 < z \leq 2.1$. Fig. 1 shows the sky distribution of 63 GRBs in this redshift range, which we retrieved from the Gamma-Ray Burst Online Index (GRBOX)[1] database as of 17 January 2021. The location and extent of the HCBGW, or simply the HCBGW region, is outlined by the celestial circle of radius $\approx 49.^\circ46$ centered at $(\alpha, \delta) \approx (212°, 46°)$. As described below, we determined this HCBGW region by using the point-radius bootstrap method, which Horváth et al. (2014, 2015, 2020) introduced to show the statistical significance of the large-scale anisotropy of GRBs at redshifts $1.6 < z \leq 2.1$.

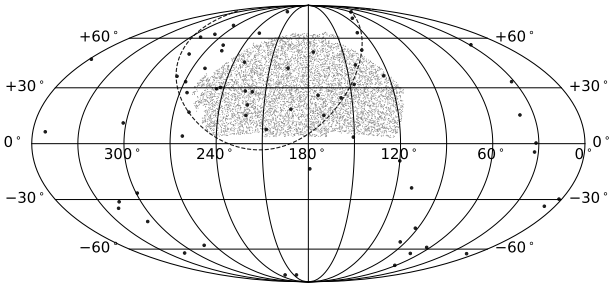

Fig. 1: The sky distribution of 63 GRBs (black dots) at redshifts $1.6 < z \leq 2.1$ in the equatorial coordinates with Mollweide projection. Small grey dots are the SDSS DR7 quasars in our volume-limited sample in the same redshift range. The HCBGW region identified by the point-radius bootstrap method, which is a spherical disk of angular radius $\approx 49.^\circ46$ centered on $(\alpha, \delta) \approx (212°, 46°)$, is outlined by the dashed line.

In the point-radius bootstrap method, one calculates the maximum number of GRBs that can be enclosed in a celestial circle of radius θ, which we denote as $N_{\rm max}(\theta)$. The same quantity is calculated for a large number of random catalogues, then the statistical significance is measured by the relative number of random catalogues with $N_{\rm max}(\theta)$ equal to or greater than that of the data. For generating random catalogues, we follow the assumption made by Horváth et al. (2014, 2015, 2020) that the sky exposure function of the GRBs is independent of redshift. Based on this assumption, a random catalogue is constructed by randomly choosing 63 celestial positions from the whole set of 488 GRBs with measured redshifts, which are taken from the GRBOX as of 17 January 2021. We generate 10000 such random catalogues.

The most statistically significant anisotropy is found at $\theta \approx 49.^\circ46$, where we obtained $N_{\rm max}(\theta) = 32$

[1] https://sites.astro.caltech.edu/grbox/grbox.php

for the GRB data while only 0.03% of random catalogues had $N_{\max}(\theta) \geq 32$. Based on this result, we define the HCBGW region as the celestial circle of radius $49\overset{\circ}{.}46$ centered at $(\alpha, \delta) \approx (212^\circ, 46^\circ)$, which contains 32 GRBs at redshifts $1.6 < z \leq 2.1$ (Fig. 1). The angular radius corresponds to the comoving length of $\approx 3.4h^{-1}$ Gpc at $z \sim 2$. Our result is generally consistent with that of Horváth et al. (2020), who used 64 GRBs in the same redshift range $1.6 < z \leq 2.1$ obtained from the GRBOX as of March 2018. Using the point-radius bootstrap method, they found the most statistically significant anisotropy at $\theta \approx 45\overset{\circ}{.}6$ ($r \equiv (1 - \cos\theta)/2 = 0.15$ in their parametrization) with $N_{\max}(\theta) = 33$, and only 0.01% of random catalogues had $N_{\max}(\theta) \geq 33$. Note that the redshift range $1.6 < z \leq 2.1$ is preselected by Horváth et al. (2014, 2015, 2020) because of its strong anisotropy in the celestial distribution of GRBs, thus the p-value $\sim 0.01\%$ mentioned above would be biased toward a lower value (Ukwatta and Woźniak 2016, Christian 2020).

Note also that the GRB sample of Horváth et al. (2020) and the one used in this work would overlap for the most part, but it is difficult to identify the difference and replicate their results. This is because the GRBOX changes its records irregularly depending on the changes of other online sources, and the update history seems not publicly available. For instance, the redshift of GRB 020819 changed from $z = 0.41$ (Jakobsson et al. 2005) to $z = 1.9621$ (Perley et al. 2017) probably soon after the publication of the latter: Table A.1 of Horváth et al. (2015) records the former value, while our query returned the latter value. However, this is not a major issue since our purpose here is not to make a strict comparison with the previous studies, but to define the HCBGW region in a way that is consistent with them.

3. QUASAR DATA

If the HCBGW is a physical structure extending over gigaparsecs, its existence should also be detectable in the quasar distribution. Quasars are known to be a good tracer of large-scale structures, and their brightness makes them particularly useful for probing the distant universe (e.g. Miller et al. 2004, Einasto et al. 2014, Song et al. 2016). In this work, we use the final version of the SDSS-I/II quasar catalogue (DR7, Schneider et al. 2010), especially its value-added version provided by Shen et al. (2011). Our sample of quasars covers a continuous region of 5837 deg^2 in the north galactic hemisphere, which includes about half of the suspected HCBGW region (Fig. 1).

There is a newer version DR16 of the SDSS quasar catalogue (Lyke et al. 2020), which compiles all quasars in the DR7 catalogue and additional data obtained in the successive SDSS-III/IV projects. We do not use this latest version since most of the SDSS-III/IV quasars in the north galactic hemisphere are in the area $120^\circ < \alpha < 250^\circ$, $30^\circ < \delta < 60^\circ$ (see, e.g. Fig. 1 of Ross et al. 2020), which only covers about a quarter of the HCBGW region. To work on a statistically homogeneous sample that covers as large a portion of the HCBGW region as possible, we use the DR7 catalogue at the expense of additional quasar data in the newer version. The sample construction is described in what follows.

First, since we are interested in the redshift range of the HCBGW, only quasars at redshifts $1.6 < z \leq 2.1$ are extracted. The uniform target condition (`UNIFORM_TARGET=1`; see Shen et al. 2011) is then applied, which leaves only quasars that were uniformly selected as spectroscopic targets by the algorithm of Richards et al. (2002). This condition is necessary for making a statistically homogeneous sample, and the selection function of such a sample is known to be nearly uniform in the sky (Shen et al. 2007, 2011).

As Shen et al. (2007) described in detail, the sky coverage of the uniform sample can be quantified as an overlapping region of rectangular targeting tiles (used for imaging) of width $2\overset{\circ}{.}5$ and circular spectroscopic tiles of radius $1\overset{\circ}{.}49$. We retrieved the tiling geometry data by querying the SDSS DR7 database via Catalog Archive Server Jobs System (CasJobs)[2]. From the entire region with uniform selection, a continuous region of ≈ 5837 deg^2 is selected for our analyses (Fig. 1). This uniform sample contains 11175 quasars at redshifts $1.6 < z \leq 2.1$, and its comoving number density is $\approx 9.7 \times 10^{-7} h^3$ Mpc^{-3}. Fig. 2 shows that the number density of the uniform sample is decreasing with redshift.

Lastly, for making a volume-limited sample whose number density is constant over redshift, the following absolute magnitude cut is applied as in Park et al. (2015):

$$M_{i,z=2} \leq 1.697z^2 - 6.895z - 19.857, \qquad (1)$$

where $M_{i,z=2}$ is the i-band absolute magnitude that is K-corrected to $z = 2$ (Richards et al. 2006). The values of $M_{i,z=2}$ are also taken from the value-added catalogue of Shen et al. (2011); we need not recalculate them because Shen et al. (2011) assumed the same cosmological parameters as those in this work. The finally obtained volume-limited sample contains $N_q = 7847$ quasars, whose comoving number density is $\approx 6.8 \times 10^{-7} h^3$ Mpc^{-3} and is nearly constant over redshift (Fig. 2).

4. FRACTAL ANALYSIS

One of the standard ways to investigate the large-scale homogeneity of the universe is to measure the homogeneity scale, denoted as $r_{\rm h}$, in the spatial distribution of cosmic objects. In this section, we perform this test for our quasar sample based on the counts-in-spheres $N(< r)$ and the fractal correlation dimension $D_2(r)$.

[2] https://skyserver.sdss.org/casjobs/

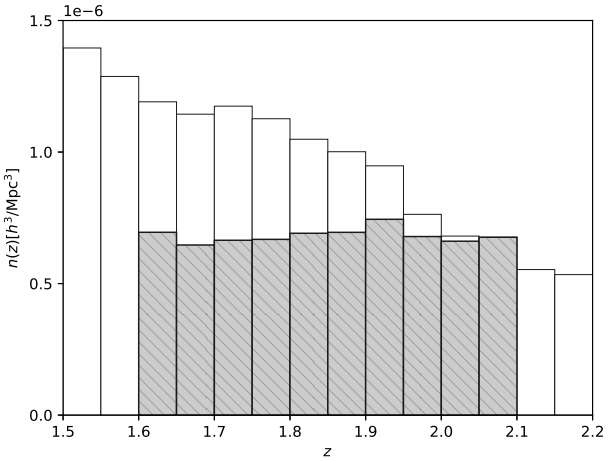

Fig. 2: The comoving number density of quasars. The empty bars are for all quasars satisfying the uniform target condition, and the shaded bars are for our volume-limited quasar sample.

4.1. Fractal correlation dimension

The fractal correlation dimension is defined as (e.g. Wu et al. 1999):

$$D_2(r) \equiv \frac{\mathrm{d}\ln N(<r)}{\mathrm{d}\ln r}, \tag{2}$$

where $N(<r)$ is the counts-in-spheres of radius r, i.e. the average number of neighbours of a cosmic object (a quasar in this work) within comoving radius r. For a homogeneous distribution in space we have $N(<r) \propto r^3$ and $D_2 = 3$, while for a fractal distribution of points that has self-similar structures on all scales, we have $N(<r) \propto r^{D_2}$ with $0 < D_2 < 3$. The latter case has been pursued by some authors as fractal cosmology (Grujic 2011, and references therein).

For a point distribution that is hierarchically clustered on small scales but homogeneous on large enough scales, which we assume in the standard cosmology (i.e. the cosmological principle), the counts-in-spheres is related to the two-point correlation function $\xi(r)$ via:

$$N(<r) = 4\pi\bar{n}\int_0^r (1+\xi(s))\, s^2 \mathrm{d}s, \tag{3}$$

where $\bar{n}$ is the average number density of the population. In this case, we have $0 < D_2(r) < 3$ for a small r due to small-scale clustering, and $D_2(r)$ approaches to the homogeneous value of 3 as r increases. Indeed, when the correlation function has a power-law form $\xi(r) = (r/r_0)^{-\gamma}$ with a correlation length $r_0 > 0$ and a slope $0 < \gamma < 3$ (e.g. Totsuji and Kihara 1969, Peebles 1980), we can calculate $D_2(r)$ analytically as:

$$D_2(r) = 3 - \frac{3\gamma}{3 + (3-\gamma)(r/r_0)^{\gamma}}, \tag{4}$$

which satisfies $D_2(0) = 3 - \gamma$ and $D_2(+\infty) = 3$. The homogeneity scale can be defined as the comoving length where $D_2(r)$ is closer to 3 than a certain threshold.

4.2. Estimation of the homogeneity scale

To correct for the survey geometry, we generate $R = 100$ random catalogues, each of which contains $N_q = 7847$ random points within the survey geometry, and define the 'scaled' counts-in-spheres (e.g. Scrimgeour et al. 2012):

$$\mathcal{N}(<r) \equiv \frac{1}{N_q}\sum_{i=1}^{N_q} \frac{N^i(<r)}{\frac{1}{R}\sum_{j=1}^{R} N^{i,j}(<r)}, \tag{5}$$

where $N^i(<r)$ is the number of neighbours of the i-th quasar within radius r, and $N^{i,j}(<r)$ is the number of points in the j-th random catalogue within radius r from the location of the i-th quasar. This approach maximizes the use of the data, but one should note that using random catalogues is equivalent to assuming homogeneity on the largest scale of the survey[3]. Since such a scale is $\approx 6.6h^{-1}$ Gpc in our case (the maximum distance between any pair of quasars), the use of random catalogues would be justified as long as we consider the scales of several hundred megaparsecs.

From the scaled counts-in-spheres we estimate the fractal correlation dimension as

$$D_2(r) = \frac{\mathrm{d}\ln\mathcal{N}(<r)}{\mathrm{d}\ln r} + 3, \tag{6}$$

where the additional term of 3 is needed since we have $\mathcal{N}(<r) \propto r^{D_2-3}$ when $N(<r) \propto r^{D_2}$. If the large-scale homogeneity postulated by the cosmological principle holds in our quasar sample, then we expect $D_2(r) \to 3$ as r increases. In this paper, we define the homogeneity scale r_h as the comoving length where $D_2(r)$ approaches the homogeneous value ($D_2 = 3$) within 1%, i.e. $D_2(r_\mathrm{h}) = 2.97$. This definition was first proposed by Scrimgeour et al. (2012) and has been commonly adopted in this field since then.

To calculate r_h, previous studies (e.g. Scrimgeour et al. 2012, Ntelis et al. 2017, Gonçalves et al. 2018a, Gonçalves et al. 2021) fit a polynomial function to the estimated values of $D_2(r)$. Since we found that a polynomial fitting yields in our case a curve that wiggles between the data points, we use instead the Eq. (4) for the fitting and calculate the solution for $D_2(r) = 2.97$:

$$r_\mathrm{h} = r_0\left(\frac{3-\gamma}{100\gamma - 3}\right)^{-\frac{1}{\gamma}}. \tag{7}$$

[3]In addition, all three-dimensional tests implicitly assume large-scale homogeneity of the universe if the comoving distances are calculated by the FLRW metric. For a completely model-independent test on the cosmological principle, see Clarkson et al. (2008).

However, the choice of fitting function does not change the general results.

The statistical errors are estimated by the jackknife resampling method (e.g. Norberg et al. 2009). For this, we split the quasar sample into $N_{\rm s} = 9$ subvolumes of approximately the same size, then create $N_{\rm s}$ jackknife samples by omitting each of the subvolumes in turn, i.e. each jackknife sample contains about $8/9 \approx 89\%$ of the quasars. We calculate $D_2(r)$ and $r_{\rm h}$ for each of the jackknife samples and estimate the covariance matrix by

$$\mathrm{Cov}(x, y) = \frac{N_{\rm s} - 1}{N_{\rm s}} \sum_{i=1}^{N_{\rm s}} (x_i - \bar{x})\,(y_i - \bar{y})\,, \qquad (8)$$

where x_i and y_i are the statistics of interest computed from the i-th jackknife sample and $\bar{x} = \sum_{i=1}^{N_{\rm s}} x_i / N_{\rm s}$.

4.3. Results and discussion

Fig. 3 shows the fractal correlation dimension $D_2(r)$ obtained from our quasar sample, where we binned the comoving distance from $30h^{-1}$ Mpc to $300h^{-1}$ Mpc in logarithmic scale. As expected from the cosmological principle, $D_2(r)$ approaches to the homogeneous value ($= 3$) at scales $r \gtrsim 100h^{-1}$ Mpc. Fitting the Eq. (4) to the derived $D_2(r)$ values for each of the jackknife samples yields $r_0 = 11.0 \pm 2.8h^{-1}$ Mpc and $\gamma = 2.49 \pm 0.56$, and the homogeneity scale Eq. (7) is estimated to be $r_h = 136 \pm 38h^{-1}$ Mpc.

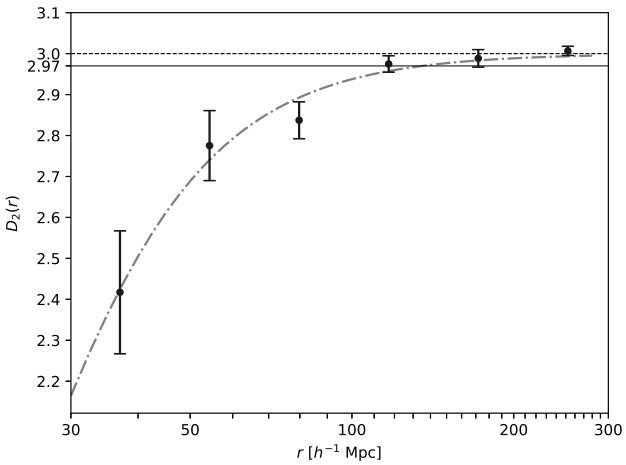

Fig. 3: The fractal correlation dimension $D_2(r)$ obtained for our uniform sample of quasars. The dash-dot curve is the best fit of the Eq. (4). The dashed and solid horizontal lines represent the homogeneous value ($= 3$) and a 1% deviation from it ($= 2.97$), respectively.

Our results are generally consistent with those of the previous studies (Nadathur 2013, Laurent et al. 2016, Gonçalves et al. 2018a, Gonçalves et al. 2021), in which $D_2(r)$ of the quasars were found to reach the homogeneous value ($= 3$) within 1% at $r \approx 80$–$130h^{-1}$ Mpc. We note that the distribution of baryonic matter (hence the quasars) is biased against the underlying dark matter distribution (e.g. Ellis et al. 2012), hence one must normally correct for the bias when confronting the results with theoretical predictions or when comparing results derived from different observations (Laurent et al. 2016, Gonçalves et al. 2018a, Gonçalves et al. 2021). However, as the bias correction is essentially a model-fitting that introduces additional parameters, here we only report the model-independent results.

Bagla et al. (2008) proposed to define the homogeneity scale as the comoving length at which $D_2(r)$ reaches the homogeneous value within one standard error (not 1%), i.e. $D_2(r_{\rm h}) = 3 - \sigma_{D_2}$. In our case, σ_{D_2} is the statistical errors estimated by the jackknife resampling method, i.e., the error bars in Fig. 3. Based on this definition and considering only shot noise for the constituents of σ_{D_2}, Yadav et al. (2010) showed that $r_{\rm h}$ is robust against the tracer bias and cosmic evolution, and derived a value $r_{\rm h} \approx 260h^{-1}$ Mpc for the concordance ΛCDM model. Since the actual measurements of $D_2(r)$ have larger errors due to contributions not considered in Yadav et al. (2010), e.g. the effects of survey boundaries and selection function, the observed homogeneity scale must be smaller than $\approx 260h^{-1}$ Mpc (Yadav et al. 2010, Scrimgeour et al. 2012, Nadathur 2013). Indeed, one sees in Fig. 3 that $|D_2(r) - 3| < \sigma_{D_2}$ at $r \gtrsim 150h^{-1}$ Mpc, thus our result obtained for the quasars in the HCBGW region is consistent with the prediction for the ΛCDM model.

5. FRIENDS-OF-FRIENDS ANALYSIS

Since the homogeneity scale is an average property of the distribution of cosmic objects, a fractal analysis may overlook giant and rare structures that can challenge the standard cosmology. Therefore, to complement the previous section, here we identify large ($> 150h^{-1}$ Mpc) quasar groups by the friends-of-friends (FoF) method and study their statistical significance following Nadathur (2013), Einasto et al. (2014) and Park et al. (2015).

5.1. Friends-of-friends cluster finding algorithm

The FoF method, also known as the single-linkage clustering method in statistics, is an algorithm for identifying groups or clusters in a point distribution. In the FoF method, any two points are grouped if the distance between them is shorter than a predetermined linking length L; if the points have already been assigned to different groups, the two groups are then merged. When the linking length is much smaller than the mean nearest neighbour separation, only identified are close pairs or compact groups that are isolated to each other. As the linking length in-

creases, the identified groups combine to form larger groups, eventually converging into a single network of filaments and walls that spans the entire volume (called the percolation).

As in Nadathur (2013), we parametrize the linking length as:

$$L = \beta \bar{r}_{\rm nn}, \tag{9}$$

where $\bar{r}_{\rm nn} = 63.8h^{-1}$ Mpc is the mean nearest neighbour separation of the quasars in our sample. Since our purpose here is to identify huge structures that are larger than the homogeneity scale, and such a structure would probably be a complex of high-density compact groups connected by relatively low-density regions, we can limit our attention to $\beta \geq 1$[4]. On the other hand, β must be smaller than a critical value β_c at which the percolation occurs . We numerically estimated β_c for our quasar sample to be $\beta_c \approx 1.65$, where about half of the quasars join several largest groups that almost span the entire volume. Since the survey boundary creates a space where no "friends" can be found, which prevents the merging of groups, β_c is slightly higher than the prediction for a homogeneous distribution in an unbounded space (≈ 1.57, Shandarin 1983). In this work, we consider the three cases of $\beta = 1, 1.25$, and 1.5.

5.2. Characterizing the statistical significance of large quasar groups

For each linking length, we identify quasar groups with two or more members, which are characterized by the richness N_g (the number of members) and size L_g (the maximum comoving distance between the members). Since we have shown in the previous section that the homogeneity scale of the quasar distribution is $r_{\rm h} = 136 \pm 38h^{-1}$ Mpc, and our interest is whether there are statistically significant structures larger than this homogeneity scale, here we only consider quasar groups with $L_g \geq 150h^{-1}$ Mpc. Due to this restriction on L_g and our choice of β described above, pairs of quasars ($L_g \leq 63.8\beta h^{-1}$ Mpc) are excluded from the analyses.

For comparison with the data, we generate 10000 random catalogues with the same number (= 7847) of points within the survey geometry. The mean nearest comoving separation for the random catalogues is $65.0h^{-1}$ Mpc, slightly larger than that for the data ($\bar{r}_{\rm nn} = 63.8h^{-1}$ Mpc) probably because of small-scale clustering of the real quasars (e.g. Vasilyev 2008). The FoF method is applied to each of the random catalogues in the same way as for the real sample.

As an indicator of large-scale homogeneity based on the FoF method, we consider the complementary cumulative distribution (CCD) of the richness of the identified FoF groups, $\phi(\geq N_g)$, which is the number of groups with richness equal to or larger than N_g; similarly, we consider the CCD of the size $\phi(\geq L_g)$. If the observed CCDs deviate significantly from those of the random catalogues, it suggests that the distribution of quasars is far from random on large scales.

For quantifying the deviation of a given CCD ϕ from the average μ computed from random catalogues, we follow Park et al. (2015) and define the statistics:

$$\chi^2 \equiv \frac{1}{X_u - X_l} \int_{X_l}^{X_u} \frac{[\phi(\geq X) - \mu(X)]^2}{\sigma(X)^2} {\rm d}X, \tag{10}$$

where X is either N_g or L_g and $\sigma(X)$ is the standard deviation of $\phi(\geq X)$ obtained from random catalogues. The lower bound of the integral is taken to be $X_l = 3$ for richness and $X_l = 150h^{-1}$ Mpc for comoving size, respectively. The upper bound is chosen such that $\mu(X_u) = 3$ (Park et al. 2015) to exclude the upper tail, for which it is meaningless to consider the average and the deviation from it.

5.3. Results and discussion

Fig. 4 shows the CCDs of richness and size of the large ($L_g \geq 150h^{-1}$ Mpc) quasar groups; our choice of the values of β enables us to cover a wide range of richness and size. The richest group identified for $\beta = 1$ ($L = 63.8h^{-1}$ Mpc) is also the largest in this case, with richness $N_g = 18$ and size $L_g \approx 281h^{-1}$ Mpc, and is comparable to the Large Quasar Groups (LQGs) discussed in Clowes and Campusano (1991) and Clowes et al. (2012). For $\beta = 1.5$ ($L = 95.8h^{-1}$ Mpc), the largest groups ($N_g \geq 100$, $L_g \gtrsim 1h^{-1}$ Gpc) are comparable to or even larger than the Huge-LQG (Clowes et al. 2013, Marinello et al. 2016). For the intermediate case with $\beta = 1.25$ ($L = 79.8h^{-1}$ Mpc), the maximum richness and size are $N_g \lesssim 50$ and $L_g \lesssim 700h^{-1}$ Mpc, respectively.

The filled areas in Fig. 4 represent 68.3%, 95.4%, and 99.7% confidence intervals derived from the 10000 random catalogues. One sees that the observed distributions of N_g and L_g are generally consistent with the expectations from a homogeneous distribution. More quantitatively, Fig. 5 shows the probability density distributions of χ^2 (Eq. 10) for richness (left panels) and comoving size (right panels) of the quasar groups derived from the random catalogues; we also plot vertical lines showing the χ^2-values for the observed CCDs. The probabilities of having $\chi^2 \geq \chi^2_{\rm obs}$ are 5.5% ($\beta = 1$), 52.9% ($\beta = 1.25$), and 96.3% ($\beta = 1.5$) for richness, and 12.1% ($\beta = 1$), 59.9% ($\beta = 1.25$), and 72.7% ($\beta = 1.5$) for comoving size, respectively. The relatively small probabilities for $\beta = 1$ are due to the intrinsic clustering of quasars on scales $< 100h^{-1}$ Mpc, which is not modeled in the random catalogues (Einasto et al. 2014, Park et al. 2015). From these results, we conclude

[4] Even if there were a huge collapsed structure larger than the homogeneity scale, an FoF analysis with $\beta = 1$ would certainly find it.

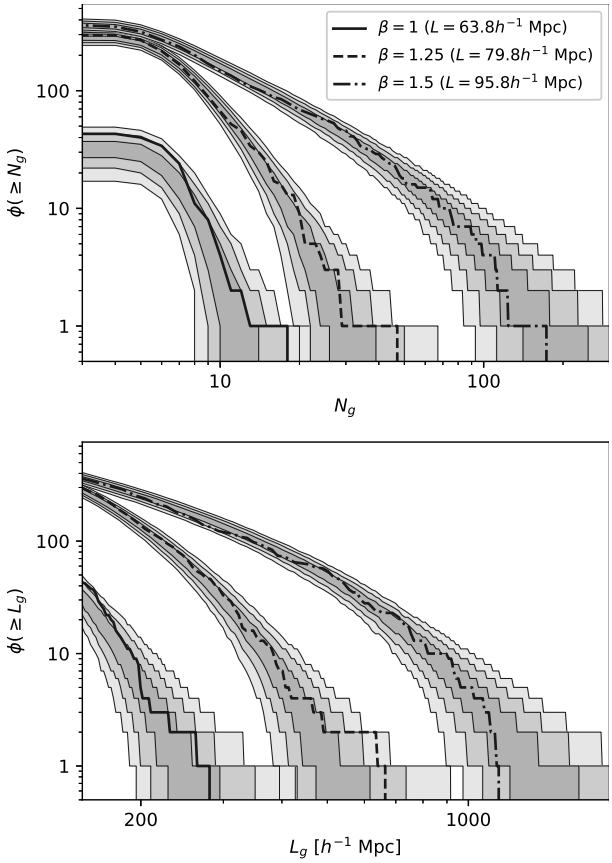

Fig. 4: The complementary cumulative distributions of the richness (upper panel) and comoving size (lower panel) of quasar groups that are identified by the FoF method, for $\beta = 1, 1.25$, and 1.5. The filled areas are 68.3%, 95.4%, and 99.7% confidence intervals derived from 10000 random catalogues.

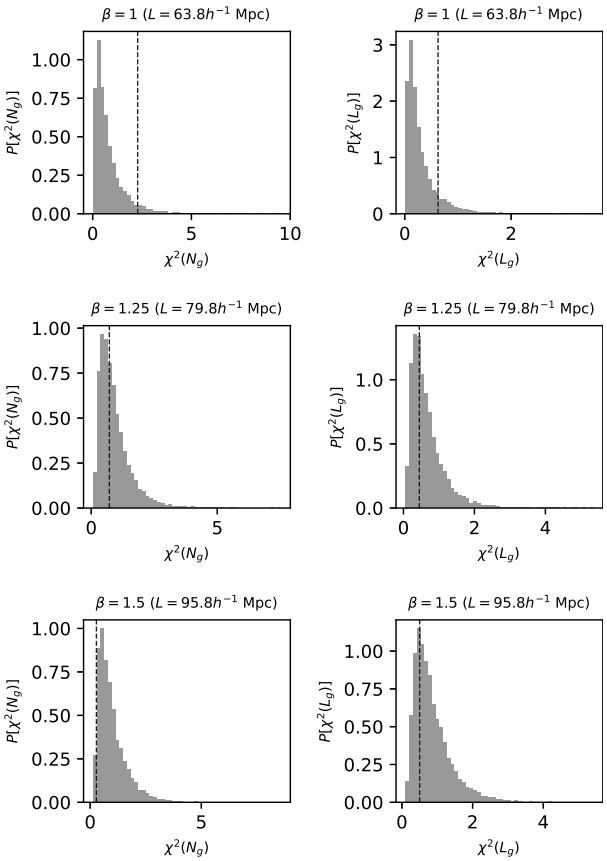

Fig. 5: The probability density distributions of χ^2 (Eq. 10) for richness N_g (left panels) and comoving size L_g (right panels) derived from 10000 random catalogues, for $\beta = 1, 1.25$, and 1.5. The dashed vertical lines represent the values of observational data.

that there are no statistically significant deviations in the overall distributions of N_g and L_g.

We also study the upper tails of CCDs, which are omitted from the previous discussion. In Fig. 4, one may notice deviations at $N_g \lesssim 20$ for $\beta = 1$, $N_g \lesssim 50$ for $\beta = 1.25$, and $L_g \gtrsim 600h^{-1}$ Mpc for $\beta = 1.25$. These features are related to the following two quasar groups, the first one being a subset of the other:

- Group I: The richest and largest group identified for $\beta = 1$, with $N_g = 18$ and $L_g \approx 281h^{-1}$ Mpc. The average location in the sky and redshift of the member quasars are $(\alpha, \delta) \approx (153.^\circ 6, 25.^\circ 9)$ and $z \approx 1.87$, respectively.

- Group II: The richest and second largest group identified for $\beta = 1.25$, with $N_g = 47$ and $L_g \approx 638h^{-1}$ Mpc. The average location in the sky and redshift of the member quasars are $(\alpha, \delta) \approx (151.^\circ 7, 25.^\circ 7)$ and $z \approx 1.88$, respectively.

Fig. 6 shows the distribution of member quasars of Group I and II, in the sky coordinates (bottom panel) and redshifts (top panel). Of the 47 quasars belonging to Group II, 18 quasars that are also members of Group I are plotted with small dark dots. The shaded area in Fig. 6 is the HCBGW region identified in Section 2; these quasar groups are almost outside the region.

The probabilities of finding, in a random catalogue, FoF groups that are richer than Group I and II are 2.7% (for $\beta = 1$) and 4.2% (for $\beta = 1.25$), respectively[5]. These may be regarded as statistically significant if a traditionally used (but often criticized) p-value threshold of 5% is adopted. However, since our analysis is based on random catalogues, in which model quasars have no correlations on small scales

[5]The probability that the second largest group for $\beta = 1.25$ is equal to or larger than Group II is even lower, 0.7%, but such an ad-hoc statistical measure should not be used without justification.

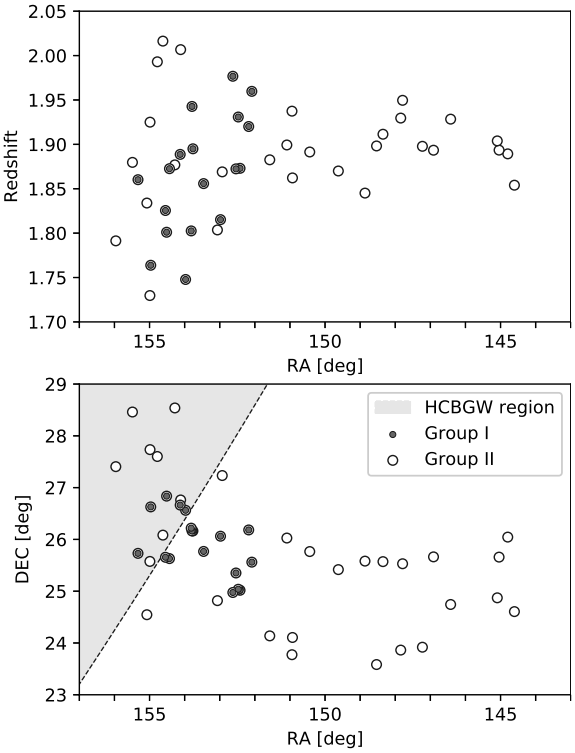

Fig. 6: The distribution of the 47 quasars belonging to the richest group identified for $\beta = 1.25$ (Group II). The small dark dots are the 18 quasars that are also belonging to the richest group for $\beta = 1$ (Group I). The shaded area in the lower panel represents the HCBGW region.

($< 100h^{-1}$ Mpc) and less chance of forming rich groups than real quasars, these probabilities would even increase if one uses more realistic mock catalogues. In any case, in the context of searching for evidence for the HCBGW, which is supposed to span several gigaparsecs, the existence of a single overdense region of several hundred megaparsecs in size is not sufficient to draw a positive conclusion.

6. CONCLUSION

The HCBGW is a gigaparsec-scale association of gamma-ray bursts (GRBs) at redshifts $1.6 < z \leq 2.1$ (Horváth et al. 2014, 2015, 2020). It has attracted attention because of its cosmological interest (Mészáros 2019, Eingorn 2016, Canay and Eingorn 2020), but whether it is a physical structure or merely an apparent pattern created by chance or other factors remains an open problem (Ukwatta and Woźniak 2016, Christian 2020, Horváth et al. 2020).

As a first attempt to search for any evidence for the HCBGW using observational data of cosmic objects other than GRBs, we analyzed the spatial distribution of quasars in the HCBGW region and tested homogeneity on large scales. Using a volume-limited, uniform sample of quasars constructed from the SDSS DR7 quasar catalogue (Schneider et al. 2010, Shen et al. 2011), we measured the homogeneity scale of the quasar distribution to be $r_{\rm h} \approx 130h^{-1}$ Mpc, consistent with the prediction for the ΛCDM model. We also showed that the richness and size distributions of large ($> 150h^{-1}$ Mpc) quasar groups identified by the FoF method are consistent with those derived from random catalogues. Although a possible overdense region of size 300–$600h^{-1}$ Mpc was identified at redshift $z \approx 1.9$, it is much smaller than the HCBGW and its statistical significance is weak.

As noted in Section 3, in this work we used the SDSS DR7 quasar catalogue in preference to the larger area covered in the sky than to include the quasar data added in the newer versions. As a result, the quasars in our sample are very sparsely distributed (with the mean nearest neighbour distance $\bar{r}_{\rm nn} = 63.8h^{-1}$ Mpc), thus one may wonder if the shot noise is too strong and obscures the presence of large-scale structures. This effect, however, would not be significant as the number density of SDSS DR7 quasars is known to correlate well with that of more densely distributed SDSS DR12 CMASS galaxies (Song et al. 2016). The effects of redshift uncertainties ($\Delta z \sim 0.004$ for the SDSS DR7 quasars; Schneider et al. 2010) and peculiar motions (typically $\lesssim 500$ km s^{-1}), which influence the comoving positions of quasars, are negligible as long as we consider the scales of $\gtrsim 70h^{-1}$ Mpc (Clowes et al. 2012, 2013, Park et al. 2015).

Our main conclusion is that there is no clear evidence for the existence of gigaparsec-scale inhomogeneities in the HCBGW region, in line with the arguments of Ukwatta and Woźniak (2016) and Christian (2020) that questioned the statistical significance of the HCBGW. As the selection function of our quasar sample is nearly uniform in the sky (Shen et al. 2007, 2011), the results of this study are statistically more reliable than those of the previous works, which only used GRB data combined from different observations (Horváth et al. 2014, 2015, 2020, Ukwatta and Woźniak 2016, Christian 2020). On the other hand, since our sample only covers about half of the HCBGW region (Fig. 1), from the present analyses we can neither prove nor disprove the existence of the HCBGW. What can be said from this study is that the HCBGW, if it exists, does not extend to the region we have examined. Studies using observational data covering a larger area are needed before a definitive conclusion can be drawn as to whether the HCBGW is a real structure.

Acknowledgements – We would like to thank the anonymous referee who carefully read the manuscript and provided very helpful comments. Some of the results in this paper have been derived using the CosmoBolognaLib C++ libraries for cosmological calculations (Marulli et al. 2016) and the astropy Python package for astronomical calculations (Astropy Col-

laboration et al. 2013, 2018). Funding for the SDSS and SDSS-II has been provided by the Alfred P. Sloan Foundation, the Participating Institutions, the National Science Foundation, the U.S. Department of Energy, the National Aeronautics and Space Administration, the Japanese Monbukagakusho, the Max Planck Society, and the Higher Education Funding Council for England. The SDSS Web Site is http://www.sdss.org/. The SDSS is managed by the Astrophysical Research Consortium for the Participating Institutions. The Participating Institutions are the American Museum of Natural History, Astrophysical Institute Potsdam, University of Basel, University of Cambridge, Case Western Reserve University, University of Chicago, Drexel University, Fermilab, the Institute for Advanced Study, the Japan Participation Group, Johns Hopkins University, the Joint Institute for Nuclear Astrophysics, the Kavli Institute for Particle Astrophysics and Cosmology, the Korean Scientist Group, the Chinese Academy of Sciences (LAMOST), Los Alamos National Laboratory, the Max-Planck-Institute for Astronomy (MPIA), the Max-Planck-Institute for Astrophysics (MPA), New Mexico State University, Ohio State University, University of Pittsburgh, University of Portsmouth, Princeton University, the United States Naval Observatory, and the University of Washington.

REFERENCES

Astropy Collaboration, Robitaille, T. P., Tollerud, E. J., et al. 2013, A&A, 558, A33
Astropy Collaboration, Price-Whelan, A. M., Sipőcz, B. M., et al. 2018, AJ, 156, 123
Bagla, J. S., Yadav, J. and Seshadri, T. R. 2008, MNRAS, 390, 829
Balázs, L. G., Bagoly, Z., Hakkila, J. E., et al. 2015, MNRAS, 452, 2236
Balázs, L. G., Rejtő, L. and Tusnády, G. 2018, MNRAS, 473, 3169
Canay, E. and Eingorn, M. 2020, PDU, 29, 100565
Christian, S. 2020, MNRAS, 495, 4291
Clarkson, C., Bassett, B. and Lu, T. H.-C. 2008, PhRvL, 101, 011301
Clowes, R. G. and Campusano, L. E. 1991, MNRAS, 249, 218
Clowes, R. G., Campusano, L. E., Graham, M. J. and Söchting, I. K. 2012, MNRAS, 419, 556
Clowes, R. G., Harris, K. A., Raghunathan, S., et al. 2013, MNRAS, 429, 2910
Einasto, M., Tago, E., Lietzen, H., et al. 2014, A&A, 568, A46
Eingorn, M. 2016, ApJ, 825, 84
Ellis, G. F. R., Maartens, R. and MacCallum, M. A. H. 2012, Relativistic Cosmology
Gonçalves, R. S., Carvalho, G. C., Bengaly, C. A. P., Carvalho, J. C. and Alcaniz, J. S. 2018a, MNRAS, 481, 5270
Gonçalves, R. S., Carvalho, G. C., Bengaly, Jr., C. A. P., et al. 2018b, MNRAS, 475, L20
Gonçalves, R. S., Carvalho, G. C., Andrade, U., et al. 2021, JCAP, 2021, 029
Grujic, P. 2011, SerAJ, 182, 1
Hogg, D. W., Eisenstein, D. J., Blanton, M. R., et al. 2005, ApJ, 624, 54
Horváth, I., Hakkila, J. and Bagoly, Z. 2014, A&A, 561, L12
Horváth, I., Bagoly, Z., Hakkila, J. and Tóth, L. V. 2015, A&A, 584, A48
Horváth, I., Szécsi, D., Hakkila, J., et al. 2020, MNRAS, 498, 2544
Jakobsson, P., Frail, D. A., Fox, D. B., et al. 2005, ApJ, 629, 45
Joyce, M., Montuori, M. and Sylos Labini, F. 1999, ApJL, 514, L5
Laurent, P., Le Goff, J.-M., Burtin, E., et al. 2016, JCAP, 11, 060
Lopez, A. M., Clowes, R. G. and Williger, G. M. 2022, arXiv:2201.06875
Lyke, B. W., Higley, A. N., McLane, J. N., et al. 2020, ApJS, 250, 8
Marinello, G. E., Clowes, R. G., Campusano, L. E., et al. 2016, MNRAS, 461, 2267
Marulli, F., Veropalumbo, A. and Moresco, M. 2016, A&C, 14, 35
Mészáros, A. 2019, AN, 340, 564
Miller, L., Croom, S. M., Boyle, B. J., et al. 2004, MNRAS, 355, 385
Nadathur, S. 2013, MNRAS, 434, 398
Norberg, P., Baugh, C. M., Gaztañaga, E. and Croton, D. J. 2009, MNRAS, 396, 19
Ntelis, P., Hamilton, J.-C., Le Goff, J.-M., et al. 2017, JCAP, 6, 019
Pan, J. and Coles, P. 2000, MNRAS, 318, L51
Park, C., Choi, Y.-Y., Kim, J., et al. 2012, ApJL, 759, L7
Park, C., Song, H., Einasto, M., Lietzen, H. and Heinamaki, P. 2015, JKAS, 48, 75
Park, C.-G., Hyun, H., Noh, H. and Hwang, J.-c. 2017, MNRAS, 469, 1924
Peebles, P. J. E. 1980, The large-scale structure of the universe
Perley, D. A., Krühler, T., Schady, P., et al. 2017, MNRAS, 465, L89
Pilipenko, S. and Malinovsky, A. 2013, arXiv:1306.3970
Richards, G. T., Fan, X., Newberg, H. J., et al. 2002, AJ, 123, 2945
Richards, G. T., Strauss, M. A., Fan, X., et al. 2006, AJ, 131, 2766
Ross, A. J., Bautista, J., Tojeiro, R., et al. 2020, MNRAS, 498, 2354
Sarkar, P., Yadav, J., Pandey, B. and Bharadwaj, S. 2009, MNRAS, 399, L128
Schneider, D. P., Richards, G. T., Hall, P. B., et al. 2010, AJ, 139, 2360
Scrimgeour, M. I., Davis, T., Blake, C., et al. 2012, MNRAS, 425, 116
Shandarin, S. F. 1983, SvAL, 9, 104

Shen, Y., Strauss, M. A., Oguri, M., et al. 2007, AJ, 133, 2222
Shen, Y., Richards, G. T., Strauss, M. A., et al. 2011, ApJS, 194, 45
Sheth, R. K. and Diaferio, A. 2011, MNRAS, 417, 2938
Song, H., Park, C., Lietzen, H. and Einasto, M. 2016, ApJ, 827, 104
Sylos Labini, F. 2011, EPL, 96, 59001
Sylos Labini, F., Vasilyev, N. L. and Baryshev, Y. V. 2009, A&A, 508, 17
Sylos Labini, F., Tekhanovich, D. and Baryshev, Y. V. 2014, JCAP, 7, 035
Totsuji, H. and Kihara, T. 1969, PASJ, 21, 221
Ukwatta, T. N. and Woźniak, P. R. 2016, MNRAS, 455, 703
Vasilyev, N. L. 2008, Ap, 51, 320
Wu, K. K. S., Lahav, O. and Rees, M. J. 1999, Natur, 397, 225
Yadav, J. K., Bagla, J. S. and Khandai, N. 2010, MNRAS, 405, 2009

ХОМОГЕНОСТ У РАСПОДЕЛИ КВАЗАРА НА ВЕЛИКИМ СКАЛАМА У ОБЛАСТИ ВЕЛИКОГ ЗИДА ХЕРКУЛ-СЕВЕРНА КРУНА

Hirokazu Fujii

Independent Researcher, Minato-ku, Tokyo, Japan
E–mail: *hirokazufujii@gmail.com*

УДК 524.7–823 + 524.8
Оригинални научни рад

У светлу скорашњих дебата о постојању структура реда величине гигапарсека мапираних помоћу гама бљескова, конкретно Великог зида Hercules-Corona Borealis (HCBGW, Херкул–Северна круна на српском), скрећемо поново пажњу на хомогеност у расподели квазара на великим скалама. Наш просторно ограничен узорак квазара на црвеним помацима $1.6 < z \leq 2.1$, добијен из 7. издања каталога квазара у прегледу неба Sloan Digital Sky Survey, покрива око половину региона за који се претпоставља да представља HCBGW. Анализирамо узорак на два компламентарна начина: фрактална анализа за добијање просечне скале хомогености и анализа "пријатељи пријатеља" за идентификовање одређених структура на великим скалама. Расподела квазара у просеку постиже хомогеност на $r_{\rm h} = 136 \pm 38\,h^{-1}\,$Mpc, а богатство и учесталост величине (у успутном референтном систему) великих ($\gtrsim 150\,h^{-1}\,$Mpc) група квазара конзистентне су са предвиђањима хомогене расподеле. Ови резултати ограничавају простирање HCBGW али нису у супротности са њиховим постојањем јер наш узорак квазара не покрива целу област HCBGW.